Atomic clock transitions in silicon-based spin qubits

Gary Wolfowicz,[1, 2, *] Alexei M. Tyryshkin,[3] Richard E. George,[1] Helge Riemann,[4] Nikolai V. Abrosimov,[4]
Peter Becker,[5] Hans-Joachim Pohl,[6] Mike L. W. Thewalt,[7] Stephen A. Lyon,[3] and John J. L. Morton[1, 8, †]

[1]London Centre for Nanotechnology, University College London, London WC1H 0AH, UK
[2]Dept. of Materials, Oxford University, Oxford OX1 3PH, UK
[3]Dept. of Electrical Engineering, Princeton University, Princeton, New Jersey 08544, USA
[4]Institute for Crystal Growth, Max-Born Strasse 2, D-12489 Berlin, Germany
[5]Physikalisch-Technische Bundesanstalt, D-38116 Braunschweig, Germany
[6]Vitcon Projectconsult GmbH, 07745 Jena, Germany
[7]Dept. of Physics, Simon Fraser University, Burnaby, British Columbia V5A 1S6, Canada
[8]Dept. of Electronic & Electrical Engineering, University College London, London WC1E 7JE, UK
(Dated: January 29, 2013)

A major challenge in using spins in the solid state for quantum technologies is protecting them from sources of decoherence. This can be addressed, to varying degrees, by improving material purity or isotopic composition [1, 2] for example, or active error correction methods such as dynamic decoupling [3, 4], or even combinations of the two [5, 6]. However, a powerful method applied to trapped ions in the context of frequency standards and atomic clocks [7, 8], is the use of particular spin transitions which are inherently robust to external perturbations. Here we show that such 'clock transitions' (CTs) can be observed for electron spins in the solid state, in particular using bismuth donors in silicon [9, 10]. This leads to dramatic enhancements in the electron spin coherence time, exceeding seconds. We find that electron spin qubits based on CTs become less sensitive to the local magnetic environment, including the presence of ^{29}Si nuclear spins as found in natural silicon. We expect the use of such CTs will be of additional importance for donor spins in future devices [11], mitigating the effects of magnetic or electric field noise arising from nearby interfaces.

Out of the various candidates for solid state qubits, spins have been of particular interest due to their relative robustness to decoherence compared to other degrees of freedom such as charge. So far, the most coherent solid state systems investigated have been the spins of well-isolated donors in bulk 28-silicon, with coherence times (T_2) of up to seconds (extrapolated) for the electron spin [1] and minutes for the nuclear spin [5], comparable to those of ion trap qubits [12, 13]. However, in practical devices, spin coherence times are likely to be limited by factors such as coupling to nearby qubits and magnetic or electric field noise from the environment. For example, cross-talk with other donors 100 nm away limits the electron spin T_{2e} to a few milliseconds [1], while a nearby interface can limit the donor electron spin T_{2e} to 0.3 ms at 5.2 K [14]. Finally, without isotopic enrichment, the 5% natural abundance of ^{29}Si limits the electron spin T_{2e} to less than 1 ms [9, 10].

An approach to creating more robust qubits is to tune free parameters of the system Hamiltonian to obtain insensitivity to specific sources of decoherence. This has been extensively used in ion trap qubits to protect against magnetic field fluctuations [12, 13], building on work on atomic clocks where hyperfine states, used as frequency standards, must remain stable against such variations. These so-called "clock transitions" (CTs) have a transition frequency (f) which is insensitive to magnetic field (B) variations, at least to first-order (in other words $df/dB = 0$). More recently, superconducting circuit qubits have also taken advantage of a tuned Hamiltonian to remain immune to charge, flux or current noise [15, 16].

Nuclear spin CTs in rare-earth dopants (nuclear spins $I > 5/2$) have been studied in the context of optical quantum memories [17, 18] leading to a 600-fold improvement of the coherence times to 150 ms, limited by second-order effects, while recent experiments on phosphorus donor nuclear spins also exploited a CT [5]. For electron spins in the solid-state, CTs remain relatively unused due in part to the requirement of a spin Hamiltonian of sufficient complexity. One of the richest single-defect spin systems is the bismuth donor in silicon (Si:Bi), which possesses an electron spin $S = 1/2$ coupled to a nuclear spin $I = 9/2$. The electron spin decoherence rates for Si:Bi have been found to follow df/dB in both natural silicon [9], and isotopically enriched ^{28}Si [19]. These results, combined with the identification of a number of CTs in the spin Hamiltonian of Si:Bi [20, 21], motivate the study of spin coherence times around CTs in Si:Bi, where $df/dB \to 0$. In this Letter, we investigate one such CT in Si:Bi, at 7.0317 GHz, using both natural silicon and ^{28}Si.

When describing the states of coupled electron and nuclear spins, two basis conventions are typically used: in the high magnetic field limit, the electron and nuclear spin projections m_S and m_I are good quantum numbers, while in the zero-field limit, the total spin F ($= I \pm S$) and its projection m_F ($= m_S + m_I$) are used. CTs are often found in an intermediate regime [22], nevertheless it is possible to categorize them as nuclear magnetic resonance (NMR)- or electron spin resonance (ESR)-type, on the basis of whether the transition couples primarily to S_x or I_x, where these are the electron and nuclear spin operators perpendicular to the applied magnetic field. The
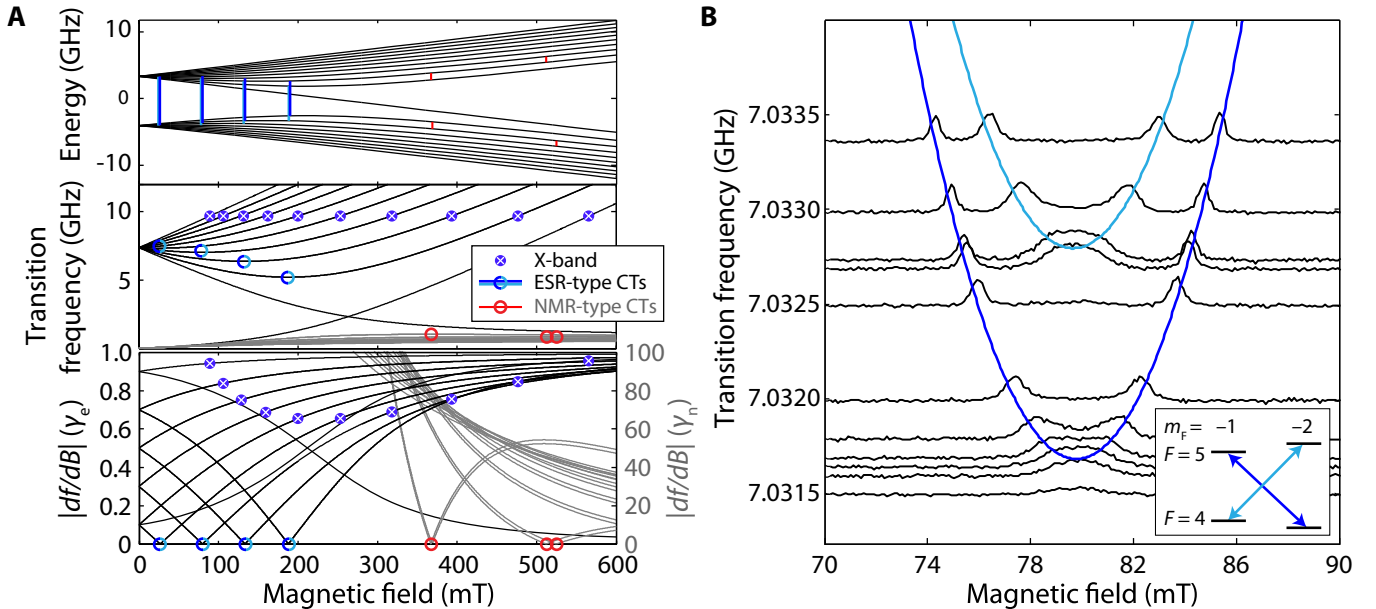
FIG. 1. **Electron spin resonance (ESR)-type clock transitions (CTs) of Si:Bi**. **A,** The eigenstate energies (top) of Si:Bi as function of magnetic field, the ESR- (black) and NMR-type (grey) transition frequencies between these states (middle), and the first-order magnetic field dependence (df/dB) of these transition frequencies (bottom). ESR-type CTs (blue lines and open circles) are found at 27, 80, 133 and 188 mT, and appear in the spectrum as doublets $\Delta F \Delta m_F = \pm 1$ separated by up to 3 MHz. NMR-type CTs are found above 300 mT (red lines and open circles). **B,** Electron spin echo-detected magnetic field sweeps around the 80 mT CT measured at microwave frequencies ≥ 7.0315 GHz. The transition probablities for $\Delta F \Delta m_F = +1$ (dark blue) and -1 (light blue) transitions are equal near the CT.

ESR-type CTs which we investigate in this manuscript involve states which are close to pure in the $|F, m_F\rangle$ basis and hence for convenience we label them according to the dominant $|F, m_F\rangle$ component (full details are given in the Supplementary Material and in Ref [20]).

For bismuth donors in silicon, NMR-type CTs can be found at high field (> 350 mT) with frequencies around 1 GHz as shown in red in Figure 1A. At low field (< 200 mT), four ESR-type CTs are present with frequencies in the range 5.2 to 7.3 GHz as shown in blue in the same figure. We will focus here on the ESR-type CTs, which possess only slightly reduced spin manipulation time compared to free electron spins as well as a large energy splitting even at low magnetic field (which has interesting applications for use in hybrid superconducting circuits [9, 23, 24]).

In the silicon samples we study here, Bi donors were introduced during crystal growth using the method developed in Ref [25], with concentrations ranging from 3.6×10^{14} cm^{-3} to 4.4×10^{15} cm^{-3}. Pulsed-ESR experiments were performed using a spectrometer based around a modified Bruker Elexsys E580 system with a ~ 7 GHz loop-gap cavity (for the CT) and 9.75 GHz dielectric resonator.

Figure 1B shows ESR spectra measured using microwave frequencies between 7.031 and 7.034 GHz, by plotting electron spin echo intensity as a function of magnetic field. The spectra show two transitions correspond-

ing to $[\{\Delta F, \Delta m_F\} = \{\pm 1, \pm 1\}]$ and $[\{\Delta F, \Delta m_F\} = \{\pm 1, \mp 1\}]$; for brevity, these transitions can be distinguished by the value of the product $\Delta F \Delta m_F = \pm 1$. Together, they offer a controllable two-qubit subsystem with low sensitivity to magnetic field fluctuations (see inset of Figure 1B).

We model the ESR spectra using an isotropic spin Hamiltonian common for group V donors in silicon:

$$H_0 = B_0(\gamma_e S_z \otimes \mathbb{1} - \gamma_n \mathbb{1} \otimes I_z) + A\vec{S}.\vec{I} \qquad (1)$$

where the two first terms correspond to the electronic (S) and nuclear (I) spin Zeeman interactions with an external field B_0 and the last term corresponds to the hyperfine coupling A. A common way to estimate Hamiltonian parameters such as the electron and nuclear gyromagnetic ratios (γ_e and γ_n) and the hyperfine constant is by measuring the magnetic field dependences of the spin transition frequencies. We use the opportunity provided by the CT (with $df/dB \to 0$) to extract a measure of the hyperfine constant $A = 1.47517(6)$ GHz with high precision, because uncertainties in the magnetic field become irrelevant. In our simulations, we additionally use the previously reported value of $\gamma_e = 27.997(1)$ GHz/T [26] and the generic value of $\gamma_n = 7$ MHz/T for ^{209}Bi [9].

Figure 1B shows that the ESR linewidth in the magnetic field domain increases around the CT: the derivative df/dB tends to zero hence its inverse, dB/df, diverges until it becomes limited by the non-linear terms
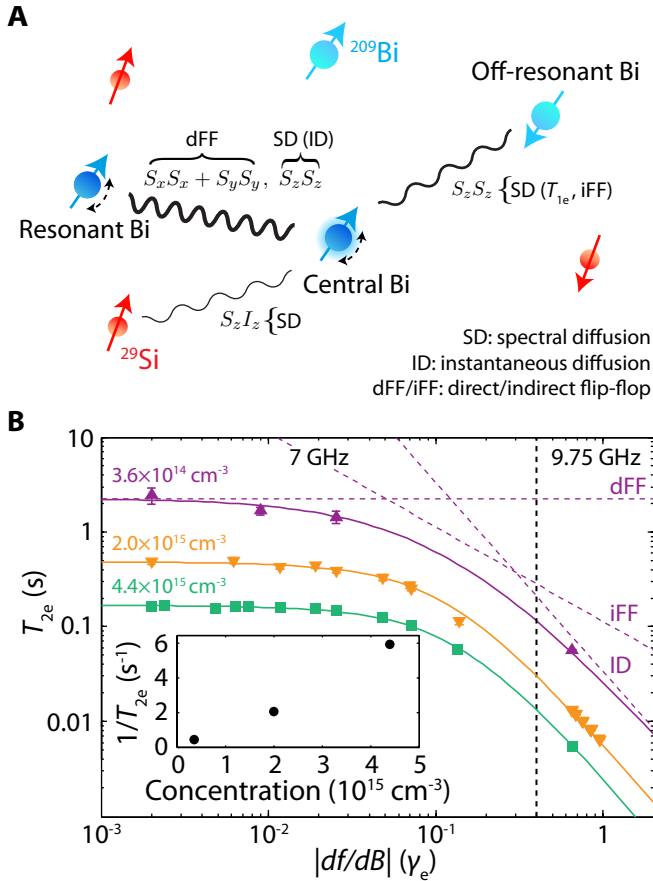
FIG. 2. **Decoherence mechanisms of Bi donors in silicon and their dependence on** df/dB. **A,** In the central spin representation, a Bi donor is coupled to neighbouring Bi donors as well as ^{29}Si spins. At the ESR CT, all spectral diffusion (SD) contributions to decoherence are essentially eliminated, leaving only the direct flip-flop term (dFF) between the central spin and a neighbouring, resonant Bi spin. **B,** T_{2e} measurements at 4.8 K show a strong dependence on df/dB, as shown for 3 different donor concentrations in ^{28}Si:Bi. Measurements close to $df/dB = \gamma_e$ were taken using the ten X-band ESR transitions, while the remaining points were taken close to the CT. For each concentration, the dependence on df/dB is modeled using contributions from ID, FF and iFF, as shown separately in dashed lines for the lowest concentration. Inset shows the limit of $1/T_{2e}$ when approaching to the exact CT as a function of donor concentration, showing a nearly linear dependence, as expected for dFF.

in $f(B_0)$. These spectra are all well fit assuming a constant linewidth in the frequency domain of 270 kHz. This linewidth can be attributed to a distribution in the hyperfine constant of around 60 kHz, using $\Delta f = \frac{df}{dA}\Delta A$ at the CT. Fourier-Transform ESR performed at a range of frequencies confirmed that the ESR linewidth in frequency domain is indeed magnetic field independent (see Supplementary Material).

We now examine the decoherence mechanisms which affect the electron spin of donors in silicon. At sufficiently low temperature (< 5 K), spin-lattice relaxation T_{1e} can be mostly neglected, and dipolar interactions ($\sim 2S_zS_z - (S_xS_x + S_yS_y)$) with neighbouring spins are the primary source of decoherence. In a central spin representation, as shown in Figure 2A, the surrounding spins can be divided into three categories: i) resonant spins affected by microwave excitation; ii) off-resonant spins of the same species, i.e. Bi spins in m_F levels not addressed by the microwaves; and iii) other spin species such as ^{29}Si. Away from CTs, the limiting factor for electron spin coherence times is spectral diffusion (SD) from the S_zS_z term of the dipolar interaction. This term can be assimilated into effective fluctuations in the magnetic field environment of the central spin. SD is independent of any frequency detuning between spins and thus is valid between the central spin and any others.

In the static case, dipolar couplings to (ii) and (iii) can be refocused with a microwave π-pulse such as in the Hahn echo sequence. However, this does not correct for the dipolar coupling between resonant spins (i) as both spins are simultaneously flipped by the π-pulse. This is called "instantaneous diffusion" (ID) and limits its T_{2e} to $\sim 10 - 100$ ms for typical donor concentrations ($> 10^{14}$ cm^{-3}) [1, 19] [27]. Furthermore, dynamic changes from spin flips in the environment cannot be refocused. At high temperature, such flips arise from phonon scattering but at low temperature, this is due to flip-flops (FF) from the $S_xS_x + S_yS_y$ term of the dipolar interaction. FF are energy conserving and as such are only relevant between spins that have similar transition frequencies. In natural silicon, the dominant decoherence mechanism is SD from ^{29}Si FF, while in isotopically enriched ^{28}Si, it arises from FF between resonant Bi spin pairs. In the latter case, we distinguish between FF which involve the central spin (direct FF, dFF), and those which do not (indirect FF, iFF).

We begin by discussing results on samples of isotopically enriched ^{28}Si (100 ppm ^{29}Si). At the CT the transition frequency is insensitive to magnetic field fluctuations in first order, so we expect SD to have little effect, leaving only the dipolar coupling between resonant spin pairs. With reference to Figure 2A, this implies then that all terms apart from dFF vanish. In Figure 2B, measurements of electron spin coherence times (T_{2e}) are shown for three different concentrations over a wide range of df/dB. The data includes values measured at X-band as well as those near the CT ($\Delta F \Delta m_F = +1$) at 79.8 mT, 7.0317 GHz. Measurements at the CT shown here were taken at 4.8 K where $T_{1e} = 9$ s, however no increase in T_{2e} was seen at lower temperature.

For each sample, enhancements of about two orders of magnitude are seen at the CT, compared to the case for a free electron g-factor, such as that of phosphorus donors. As shown in Figure 2B, the dependence of the measured T_{2e} on df/dB arises from two factors: the effect on ID, and on iFF. ID has a known quadratic dependence on the
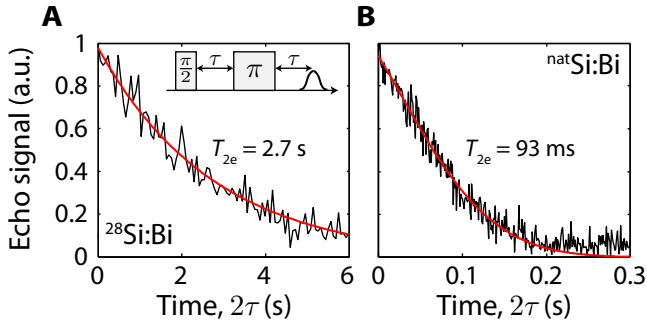
FIG. 3. **Hahn echo decay at the CT. A,** ^{28}Si:Bi at 4.3 K with a Bi concentration of 3.6×10^{14} cm^{-3}. **B,** ^{nat}Si:Bi at 4.8 K with a Bi concentration of 10^{15} cm^{-3}. The decay in natural Si is a stretched exponential, and therefore T_{2e} is defined as the time when the amplitude reaches $1/e$. Magnitude detection was used to eliminate instrumental noise, likely due to phase noise in the microwave source.

gyromagnetic ratio of the central spin [19, 28], and becomes a negligible effect for $df/dB < 0.1\gamma_e$. Indirect FF dephase the central spin through the $S_z S_z$ term, giving a linear dependence of T_{2e} on df/dB. Direct FF, on the other hand, are not eliminated at the CT, and provide an upper bound on T_{2e} for a given donor spin concentration, as plotted in the inset of Figure 2B. For the lowest concentration sample, electron spin coherence times of up to 2.7 s were measured from simple two-pulse Hahn echo decays, as shown in Figure 3A.

We now turn to measurements on Bi-doped natural silicon (^{nat}Si:Bi), which has 5% ^{29}Si. Away from the CT the effect of the ^{29}Si ($I = 1/2$) is both to broaden the ESR linewidth to about 0.4 mT (equivalent to 12 MHz in the frequency domain for a free electron) due to unresolved ^{29}Si hyperfine, as well as to limit the T_{2e} to about 0.8 ms due to SD [9]. At the CT we find that the ESR linewidth reduces to 500 kHz (see Supplementary Material), within a factor of two of the value for enriched ^{28}Si material, while T_{2e} increases by over two orders of magnitude to about 90 ms (Figure 3B). The effect of the suppression of SD around the CT has been simulated for ^{nat}Si:Bi using cluster expansion methods [29], though further refinements are required in the simulation before a quantitative comparison can be made. The stretched-exponential decay implies that T_{2e} is still limited at 93 ms by SD from ^{29}Si due to the second order term ($d^2 f/dB^2 \neq 0$). For modest ^{28}Si enrichment (e.g. [^{29}Si] ≈ 1000 ppm), T_{2e} should already exceed seconds, and indeed there may be an optimal ^{28}Si purity above which T_{2e} at the CT drops, due to the role of ^{29}Si or ^{30}Si in detuning otherwise-identical spins [30].

We have shown how CTs in Si:Bi can be used to produce magnetic field-insensitive spin qubits with directly measured coherence times of several seconds. Such qubits would be insensitive to magnetic field noise arising, for example, from fluctuating dangling-bond spins at the

Si/SiO$_2$ interface. Conversely, if electric field noise is dominant, this can couple to donor spins via the hyperfine interaction and cause decoherence. Again, CTs can be designed to be immune from electric charge noise by selecting points where $df/dA \rightarrow 0$ (see Supplementary Material). Through the use of CTs, it is likely that the seconds-long electron spin coherence times measured in the bulk can be harnessed for spins in practical quantum devices.

* gary.wolfowicz@materials.ox.ac.uk
† jjl.morton@ucl.ac.uk
[1] A. M. Tyryshkin *et al.*, Nature Materials **11**, 143 (2012).
[2] G. Balasubramanian *et al.*, Nature materials **8**, 383 (2009).
[3] L. Viola and S. Lloyd, Physical Review A **58**, 2733 (1998).
[4] H. Bluhm *et al.*, Nature Physics **7**, 109 (2011).
[5] M. Steger *et al.*, Science (New York, N.Y.) **336**, 1280 (2012).
[6] P. C. Maurer *et al.*, Science (New York, N.Y.) **336**, 1283 (2012).
[7] J. Bollinger, J. Prestage, W. Itano, and D. Wineland, Physical Review Letters **54**, 1000 (1985).
[8] P. Fisk *et al.*, IEEE Transactions on Instrumentation and Measurement **44**, 113 (1995).
[9] R. E. George *et al.*, Phys. Rev. Lett. **105**, 67601 (2010).
[10] G. W. Morley *et al.*, Nature Materials **9**, 725 (2010).
[11] J. J. Pla *et al.*, Nature **489**, 541 (2012).
[12] P. Haljan *et al.*, Physical Review A **72**, 062316 (2005).
[13] C. Langer *et al.*, Physical Review Letters **95**, 060502 (2005).
[14] T. Schenkel *et al.*, Applied Physics Letters **88**, 112101 (2006).
[15] D. Vion *et al.*, Science (New York, N.Y.) **296**, 886 (2002).
[16] J. Koch *et al.*, Physical Review A **76**, 042319 (2007).
[17] J. Longdell, A. Alexander, and M. Sellars, Physical Review B **74**, 195101 (2006).
[18] D. McAuslan, J. Bartholomew, M. Sellars, and J. Longdell, Physical Review A **85**, 032339 (2012).
[19] G. Wolfowicz *et al.*, Physical Review B **86**, 245301 (2012).
[20] M. Mohammady, G. W. Morley, and T. S. Monteiro, Phys. Rev. Lett. **105**, 067602 (2010).
[21] M. H. Mohammady, G. W. Morley, A. Nazir, and T. S.

Monteiro, Phys. Rev. B **85**, 094404 (2012).

[22] G. W. Morley *et al.*, Nature Materials **11**, 1 (2012).

[23] D. Schuster *et al.*, Phys. Rev. Lett. **105**, 140501 (2010).

[24] Y. Kubo *et al.*, Phys. Rev. A **85**, 012333 (2012).

[25] H. Riemann, N. Abrosimov, and N. Noetzel, ECS Transactions **3**, 53 (2006).

[26] G. Feher, Phys. Rev. **114**, 1219 (1959).

[27] By reducing the microwave power and effectively flipping only a small part of the resonant spins, it is possible to obtain an extrapolation of coherence times in the limit of no ID [31, 32]. However, it is not a solution to overcoming the effect of ID in practice.

[28] A. Schweiger and G. Jeschke, *Principles of pulse electron paramagnetic resonance* (Oxford University Press, Oxford, 2001).

[29] S. J. Balian *et al.*, Phys. Rev. B **86**, 104428 (2012).

[30] W. Witzel *et al.*, Physical Review Letters **105**, 187602 (2010).

[31] J. Klauder and P. Anderson, Physical Review **125**, 912 (1962).

[32] K. Salikhov, Journal of Magnetic Resonance (1969) **42**, 255 (1981).

Supplementary Material

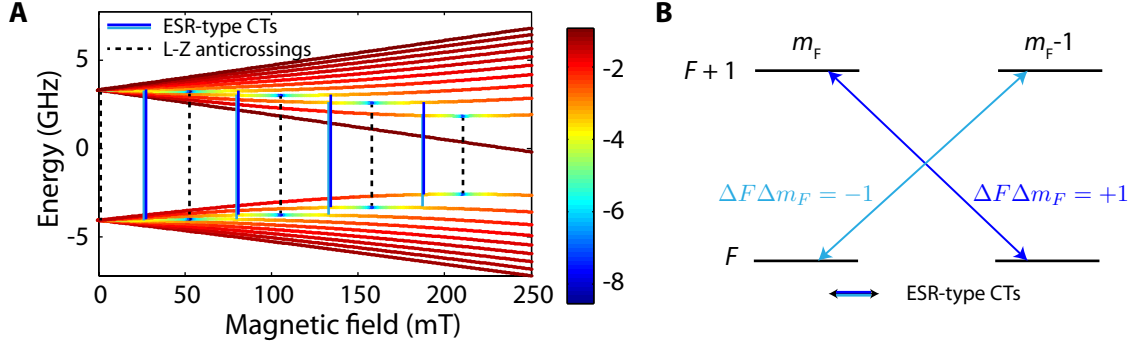## ESR- AND NMR-TYPE MAGNETIC FIELD "CLOCK" TRANSITIONS (CT)

FIG. 1. **Description of ESR-type CTs. A,** The eigenstate energies of Si:Bi as function of magnetic field. The color scale shows the logarithmic distance to pure Bell states (Landau-Zener (L-Z) anticrossings) in the $|m_S, m_I\rangle$ basis, defined as $\log(|\theta - \pi/4|)$ for an eigenstate $|\Phi\rangle = \cos(\theta)\left|\mp\frac{1}{2}, m_I \pm \frac{1}{2}\right\rangle \pm \sin(\theta)\left|\pm\frac{1}{2}, m_I \mp \frac{1}{2}\right\rangle$. The Bell state at 0 mT is barely visible here due to degeneracy. **B,** ESR-type CTs with $\Delta F \Delta m_F = +1$ in dark blue and -1 in light blue. The four involved eigenstates, which are two pairs of hyperfine coupled states in the $|m_S, m_I\rangle$ basis, form a subspace of the Hilbert space.

Below we discuss the general requirements for ESR and NMR-type CTs for systems with electron spin $S = 1/2$ and nuclear spin I and assuming an isotropic hyperfine coupling, with a particular focus on Group V donors in silicon. This letter is the first measurement of ESR-type CTs to our knowledge, though they have been theoretically described by Mohammady *et al.* [1, 2] for donors in Si, in particular Bi. On the other hand, NMR-type CTs have been used in various systems in the past [3, 4], including in phosphorus donors in silicon [5], to reduce sensitivity to magnetic field inhomogeneities (i.e. increase frequency resolution) or to increase nuclear coherence times.

In the basis of the electron and nuclear spin $|m_S, m_I\rangle$, the isotropic hyperfine interaction $(A\vec{I} \cdot \vec{S})$ couples pairs of states within the Hilbert space such that $[\Delta m_S = \pm 1, \Delta m_I = \mp 1]$. In the strongly coupled electron-nuclear spin basis $|F, m_F\rangle$ ($F = I \pm S$, $m_F = m_S + m_I$), these pairs of states share the same m_F value. When the static magnetic field is increased, the Zeeman energy rises to the same order of magnitude as the hyperfine interaction, resulting

in avoided Landau-Zener crossings between states with $m_F \leq 0$ as shown in Figure 1A. ESR-type CTs are located between pairs of these avoided crossings.

At the intermediate fields relevant to CTs and Landau-Zener anticrossing, the eigenstates can be expressed either as being close to Bell states in the $|m_S, m_I\rangle$ basis, or still quite pure in the $|F, m_F\rangle$ basis. For example, the CT at 7.0317 GHz, explored in the main text, connects the following pairs of states:

$$-0.74 \left| \frac{1}{2}, -\frac{5}{2} \right\rangle + 0.67 \left| -\frac{1}{2}, -\frac{3}{2} \right\rangle \Leftrightarrow 0.74 \left| \frac{1}{2}, -\frac{3}{2} \right\rangle + 0.67 \left| -\frac{1}{2}, -\frac{1}{2} \right\rangle \quad \text{in the } |m_S, m_I\rangle \text{ basis}$$

$$0.99 |4, -2\rangle + 0.15 |5, -2\rangle \Leftrightarrow -0.15 |4, -1\rangle + 0.99 |5, -1\rangle \quad \text{in the } |F, m_F\rangle \text{ basis}$$

Hence, for convenience, we refer to these states by the dominant term in the $|F, m_F\rangle$ basis (i.e. $|4, -2\rangle$ and $|5, -1\rangle$ in the example above). The $\Delta F \Delta m_F = +1$ and $\Delta F \Delta m_F = -1$ CTs are each transitions between one state of the first Landau-Zener crossing to a second state of the second crossing, forming a 4-dimensional subspace of the Hilbert space (Figure 1B).

For non-integer [integer] values of I, there are $I + 1/2$ [I] Landau-Zener anticrossings and consequently $2(I - 1/2)$ [$2I$] ESR-type CTs. The minimum complexity required is thus a nuclear spin $I \geq 1$ to have at least two pairs of hyperfine coupled states, which is not the case for phosphorus donors (^{31}P has $I = 1/2$).

Arsenic (^{75}As, $I = 3/2$) and antimony (^{121}Sb, $I = 5/2$ and ^{123}Sb, $I = 7/2$) have sufficient nuclear spin to permit ESR-type CTs, however the hyperfine coupling is relatively weak ($A \sim$ 198, 186 and 101 MHz, respectively), so the avoided crossings are found at low magnetic field and transition frequencies (see Table I). Bismuth ^{209}Bi with $I = 9/2$ and $A = 1.475$ GHz is thus the optimal Group V donor in silicon from the point of view of CTs, possessing four of them at GHz frequencies.

	^{75}As ($I=3/2$)	^{121}Sb ($I=5/2$)		^{123}Sb ($I=7/2$)			^{209}Bi ($I=9/2$)			
$\Delta F = +1, m_F =$	$-1 \leftrightarrow 0$	$-1 \leftrightarrow 0$	$-2 \leftrightarrow -1$	$-1 \leftrightarrow 0$	$-2 \leftrightarrow -1$	$-3 \leftrightarrow -2$	$-1 \leftrightarrow 0$	$-2 \leftrightarrow -1$	$-3 \leftrightarrow -2$	$-4 \leftrightarrow -3$
Magnetic field (mT)	3.8	3.4	10.4	1.8	5.5	9.3	26.6	79.8	133.3	187.8
Frequency (GHz)	0.384	0.552	0.482	0.403	0.376	0.314	7.338	7.032	6.372	5.214

TABLE I. **Summary of ESR-type magnetic-field CTs in donors in silicon.** CTs exist in pairs ($\Delta F \Delta m_F = \pm 1$) separated by less than 0.15 mT in magnetic field and 3 MHz in frequency. Phosphorus does not possess any CT due to its small nuclear spin ($I = 1/2$).

As $df/dB \to 0$, the next figure of merit is the electron transition probability amplitude,

which is always 50% of the high field limit for ESR-types. This means that manipulation times are only slightly reduced while electron coherence times T_{2e} are drastically increased. Conversely, as flip-flops between two donor electron spins follow the square of this probability amplitude, the flip-flopping rate remains strong, limiting T_{2e} as observed and explained in the main text.

NMR-type CTs occur at strong magnetic field (in Si:Bi, 0.3 T $< B_0 <$ 5 T, from $m_I = -9/2$ at low field to $m_I = 9/2$ at high field) and as such are transitions between quasi-pure states in the (m_S, m_I) basis. NMR-type CTs possess a change in nuclear spin state of $\Delta m_I = 1$ and can be manipulated in a conventional electron nuclear double resonance (ENDOR) or NMR experiment. Amongst the NMR-type CTs, those at higher magnetic fields have a smaller electron spin component. This leads to a reduced coupling to the environment, but also increased spin manipulation times, converging to that of a regular NMR transition (typically $\sim 10~\mu$s).

ESR LINEWIDTHS

Measurements of spin linewidths provide important details regarding the spin environment, yielding information on crystalline defects and strains amongst other properties. Line broadening arises from a variation in either the hyperfine interaction (ΔA) or the magnetic field (ΔB) (or g-tensor) across the sample. They can either be measured in a magnetic field-swept spectrum where (to first order):

$$\Delta B_{Total} = \Delta B + \frac{dB}{df}\frac{df}{dA}\Delta A \tag{1}$$

or in Fourier-Transform (FT) ESR where the FT of the free induction decay after a $\pi/2$ rotation gives the spectrum in the frequency domain. In this case, (to first order):

$$\Delta f = \frac{df}{dB}\Delta B + \frac{df}{dA}\Delta A \tag{2}$$

At the CT where $dB/df \to \infty$, the linewidth in the magnetic field domain broadens strongly until it becomes limited by the second order dependence on magnetic field. Both ΔB and ΔA can be identified by varying the transition frequency and fitting numerically knowing $\frac{dB}{df}\frac{df}{dA}$. To confirm that this change in linewidth is strictly related to the term df/dB, we can make use of the FT ESR technique which simplifies at the CT to $\Delta f = \frac{df}{dA}\Delta A$, where
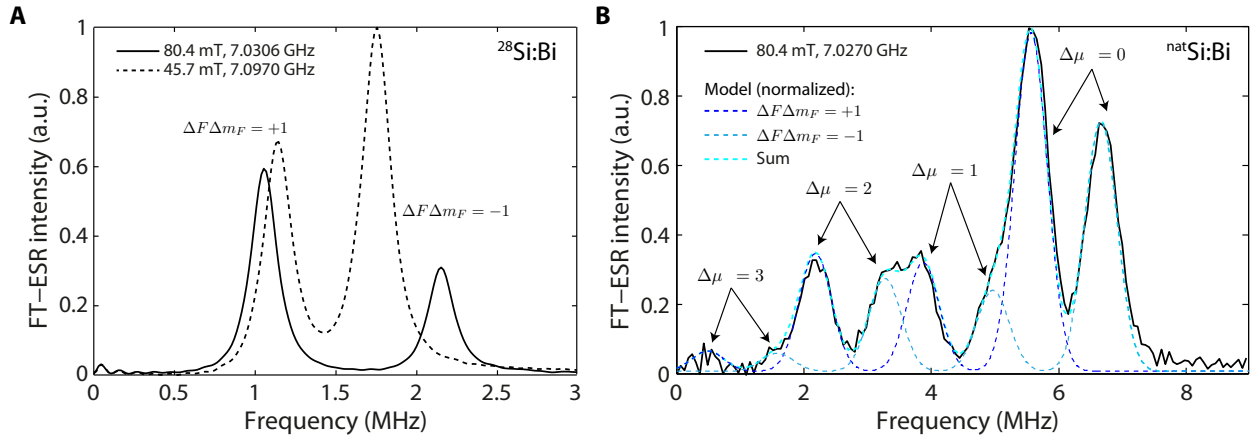
FIG. 2. **FT-ESR around the CT.** Each spectrum is the FT of the free induction decay taken using a microwave frequency slightly below resonance (values given in legend). **A,** For the case of ^{28}Si:Bi, we observe two peaks in the ESR spectrum around the CT, corresponding to the transitions $\Delta F \Delta m_F = \pm 1$. Spectra are shown as measured at two settings of magnetic field/microwave frequency. In the magnetic field domain, the ESR linewidths in these two cases are 1.6 mT close to the CT and 0.07 mT farther away (see Figure 1 of the main manuscript), however in the frequency domain as shown above, the ESR linewidths are constant. **B,** In $^{\mathrm{nat}}$Si:Bi, these two primary ESR transitions are further split into sub-peaks, corresponding to a mass-effect from nearest neighbour Si atoms. Each shift of one neutron mass ($\Delta\mu$) yields a shift of -1.7 MHz in transition frequency (or 0.024% change in the hyperfine coupling A). Dashed lines show simulated peaks whose intensity is calculated from a trinomial distribution of ^{30}Si, ^{29}Si and ^{28}Si isotopes in $^{\mathrm{nat}}$Si (with respective concentration 3.1%, 4.7% and 92%). As the FT-ESR is derived from the free induction decay, the intensities are normalized by the FT of the inhomogeneous decay $T_{2\mathrm{e}}{}^{*}$ (Lorentzian) and the cavity bandwidth.

df/dA is quasi-constant around the CT. In Figure 2A, the linewidth is indeed constant about 270 kHz.

In natural silicon, the elimination of the ΔB term dramatically reduces the ESR linewidth. Away form the CT (e.g. at X-band), ΔB is normally around 4 G due to unresolved coupling to ^{29}Si nuclear spins. In the frequency domain, this would be equivalent to nearly 12 MHz, hiding multiple spectral features. First, the two transitions $\Delta F \Delta m_F = \pm 1$ would not be resolvable. Second, as show in Figure 2B, we observe several other peaks (absent in isotopically pure ^{28}Si samples) which arise from variations in the hyperfine coupling

4

due to the total mass of nearest-neighbour silicon atoms (^{28}Si, ^{29}Si and ^{30}Si). This effect is described in full detail, including ENDOR experiments, in a forthcoming work [6].

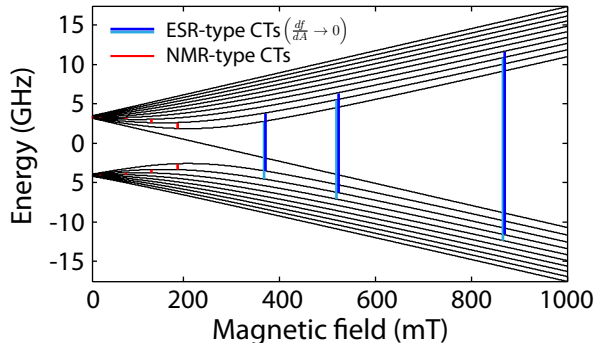## ELECTRIC FIELD CLOCK TRANSITIONS

FIG. 3. **Clock transitions in Si:Bi where $df/dA = 0$ which should be robust to electric field noise.** Both ESR- and NMR-type CTs can be observed, as for magnetic-field CTs. One further ESR-CT is found at higher magnetic fields (2.6 T, not shown).

In the experiments reported in the main text, CTs were used to reduce the sensitivity of electron spin to magnetic field variations, as quantified by df/dB. While magnetic field noise is indeed the main decoherence mechanism in bulk materials, this may not be the case in nanoscale devices where the electric field at interfaces could couple strongly with both the donor electron and nuclear spins through the hyperfine interaction (and also, to lesser extent, through a modulation in the electron spin g-factor). The sensitivity of a spin to this effect can be quantified by the gradient of the frequency with respect to the hyperfine constant df/dA, combined with values for the DC Stark effect for donors in silicon (which for Group V donors is in the order of 10^{-3} μm^2/V^2, as a fractional change in the hyperfine coupling [7, 8]). Those CTs which will be most robust to electric field noise ($df/dA \rightarrow 0$) are identified in Si:Bi in Figure 3 and in Table II for all Group V donors in silicon.

In practice, both magnetic and electric field fluctuations will participate to the donor spin decoherence. There will thus be an optimal CT, at a specific magnetic field and frequency, where the coherence time would be maximum. For example, the magnetic field CT near 188 mT in Bi has the lowest value of df/dA out of the four possible CTs. In other scenarios, it might be advantageous to minimise the inhomogeneous broadening as much as possible

	^{75}As $(I = 3/2)$	^{121}Sb $(I = 5/2)$		^{123}Sb $(I = 7/2)$			^{209}Bi $(I = 9/2)$			
$\Delta m_S = +1, m_I =$	$-1/2$	$-1/2$	$-3/2$	$-1/2$	$-3/2$	$-5/2$	$-1/2$	$-3/2$	$-5/2$	$-7/2$
Magnetic field (mT)	53	117	39	114	38	23	2607	868	519	369
Frequency (GHz)	1.43	3.21	0.92	3.17	0.98	0.49	72.64	23.18	12.57	7.30

TABLE II. **Summary of ESR-type electric-field CTs in donors in silicon.** At the given magnetic fields, the electron and nuclear spins are weakly coupled and the eigenstates must thus be expressed in the $|m_S, m_I\rangle$ basis. The $[\Delta m_S = \pm 1, \Delta m_I = \mp 2]$ $(\Delta F \Delta m_F = -1)$ transitions are nearly completely forbidden here; they would have been found at the same magnetic field as the $[\Delta m_S = \pm 1, \Delta m_I = 0]$ $(\Delta F \Delta m_F = +1)$ transitions, but separated by less than 40 MHz in frequency.

(e.g. for coupling a spin ensemble to a microwave resonator), and this would also require different optimal operating points within the Hilbert space of the bismuth electron and nuclear spins.

———————

[1] M. Mohammady, G. W. Morley, and T. S. Monteiro, Phys. Rev. Lett. **105**, 067602 (2010).

[2] M. H. Mohammady, G. W. Morley, A. Nazir, and T. S. Monteiro, Phys. Rev. B **85**, 094404 (2012).

[3] W. Hardy, A. Berlinsky, and L. Whitehead, Physical Review Letters **42**, 1042 (1979).

[4] J. Longdell, A. Alexander, and M. Sellars, Physical Review B **74**, 195101 (2006).

[5] M. Steger *et al.*, Journal of Applied Physics **109**, 102411 (2011).

[6] A. Tyryshkin *et al.*, in preparation (2013).

[7] F. Bradbury *et al.*, Physical Review Letters **97**, 176404 (2006).

[8] R. Rahman *et al.*, Physical Review Letters **99**, 36403 (2007).